

UKAEA-CCFE-PR(23)144

M. Valovič, A. Boboc, P Carvalho, I Carvalho, L. Garzotti, F. Köchl, J C Lowry, S Aleiferis, C Maggi, P Blatchford, M. Fontdecaba Climent, L. Frassinetti, C. Olde, R. B. Morales, S Nowak, E. de la Luna, F Rimini, Z Stancar, S. Silburn, G Tvalashvili, M. Brix, M. Vecsei, D. Dunai, D. Réfy, the JET team

# **Control of plasma density and isotope mix by peripheral fuelling pellets in JET D-T experiments**

Enquiries about copyright and reproduction should in the first instance be addressed to the UKAEA Publications Officer, Culham Science Centre, Building K1/O/83 Abingdon, Oxfordshire, OX14 3DB, UK. The United Kingdom Atomic Energy Authority is the copyright holder.

The contents of this document and all other UKAEA Preprints, Reports and Conference Papers are available to view online free at [scientific-publications.ukaea.uk/](https://scientific-publications.ukaea.uk/)

# **Control of plasma density and isotope mix by peripheral fuelling pellets in JET D-T experiments**

M. Valovič, A. Boboc, P Carvalho, I Carvalho, L. Garzotti, F. Köchl,  
J C Lowry, S Aleiferis, C Maggi, P Blatchford, M. Fontdecaba  
Climent, L. Frassinetti, C. Olde, R. B. Morales, S Nowak, E. de la  
Luna, F Rimini, Z Stancar, S. Silburn, G Tvalashvili, M. Brix, M.  
Vecsei, D. Dunai, D. Réfy, the JET team



# Control of plasma density and isotope mix by peripheral fuelling pellets in JET D-T experiments

M. Valovič<sup>1</sup>, A. Boboc<sup>1</sup>, P Carvalho<sup>1</sup>, I Carvalho<sup>2</sup>, L. Garzotti<sup>1</sup>, F. Köchl<sup>3</sup>, J C Lowry<sup>1</sup>, S Aleiferis<sup>1</sup>, C Maggi<sup>1</sup>, P Blatchford<sup>1</sup>, M. Fontdecaba Climent<sup>4</sup>, L. Frassinetti<sup>5</sup>, C. Olde<sup>1</sup>, R. B. Morales<sup>1</sup>, S Nowak<sup>6</sup>, E. de la Luna<sup>4</sup>, F Rimini<sup>1</sup>, Z Stancar<sup>1</sup>, S. Silburn<sup>1</sup>, G Tvalashvili<sup>1</sup>, M. Brix<sup>1</sup>, M. Vecsei<sup>7</sup>, D. Dunai<sup>7</sup>, D. Réfy<sup>7</sup> and the JET team\*

<sup>1</sup>United Kingdom Atomic Energy Authority, Culham Science Centre, Abingdon, Oxon, OX14 3DB, UK

<sup>2</sup>Instituto de Plasmas e Fusão Nuclear, Instituto Superior Técnico, Universidade de Lisboa, 1049-001 Lisboa, Portugal

<sup>3</sup>Fusion@ÖAW, Atominstitut, TU Wien, Stadionallee 2, A-1020 Vienna, Austria

<sup>4</sup>Laboratorio Nacional de Fusión, Ciemat, 28040 Madrid, Spain

<sup>5</sup>KTH Royal Institute of Technology, TEKNIKRINGEN 31, Sweden

<sup>6</sup>Institute for Plasma Science and Technology, CNR, via R. Cozzi 53, 20125 Milano, Italy

<sup>7</sup>Centre for Energy Research, Budapest, Hungary

\*\*See the author list in J. Mailloux et al 2022 Nucl. Fusion 62 042026

E-mail: martin.valovic@ukaea.uk

Received xxxxxx

Accepted for publication xxxxxx

Published xxxxxx

## Abstract

A dataset of baseline deuterium-tritium (D-T) plasmas with peripheral HFS fuelling pellets has been produced on JET, in order to mimic the situation in ITER. During the pellet ablation phase prompt particle losses due to pellet triggered ELMs can be detected. Regarding pellet deposition, the data indicate that the plasmoids drift velocity might be smaller than predicted by the HPI2 code. Post pellet particle losses are controlled by transient L-mode phases triggered by ELMs. The ratio of post-pellet particle flux to heat flux is similar to that in previous pellet fuelling experiments on AUG and JET.

Keywords: tokamak, pellets, JET D-T plasma, particle losses

## 1. Introduction

In tokamak fusion reactors like ITER the plasma density and isotope mix has to be controlled by injection of cryogenic deuterium and tritium pellets as gas fuelling will be limited to the very edge of the plasma. This is already seen on JET H-mode plasmas where above a certain gas level gas acts as an Edge Localised Modes (ELMs) controller rather than density controller [1]. High temperature at the plasma periphery expected in ITER at full current and high Q operation means that even with the largest pellet available the deposition of pellets will be quite shallow. Simulations show that these fuelling size pellets (90mm<sup>3</sup>) will deposit their material

around  $r/a \sim 0.8$  [2]. Pellet fuelling access to the core relies on favourable redistribution of pellet material by grad-B drift when pellets are injected from the high field side (HFS) of the plasma [3]. Without such drift the penetration of the pellet fuelling will be limited to the pedestal region  $r/a > 0.95$ . (Note that in addition to fuelling HFS pellets ITER will have smaller pellets (17mm<sup>3</sup>) used for ELM control with injection from both the HFS and the low field side (LFS) of the plasma).

The dataset of plasmas with ITER-like fuelling pellets is very limited. The reason is that in order to match the ratio of pellet atoms to plasma ions (7% in ITER) it means a millimeter size pellets in medium size tokamak, which is

difficult to deliver [4]. Due to its plasma size it is the unique property of JET that it is possible to match the relative pellet size to those which will be used for fuelling ITER. Simultaneously high pedestal parameters on JET determine the where the ablation of the pellets will take place, in particular leading to a shallow deposition similar to that in ITER.

In addition to ITER-like pellet size, JET can use pellets to control the D-T ratio similar to ITER's situation. The only difference is that in JET the pellet injector can operate only with deuterium pellets while in ITER both deuterium and tritium will be delivered by pellets [5]. Nevertheless the ITER-like pellet deposition profile achieved in high-performance H-mode plasmas in JET during the recent deuterium and tritium campaign (DTE2) has offered the unique opportunity to test the use of pellets to control the D-T ratio close to 50%-50%, similar to the situation in ITER.

This work is aimed to reduce the gaps in the data in both directions, fuelling and isotope control. The focus is on collection and presentation of experimental data for the purpose of density and isotope control under condition relevant to ITER's situation. Such data then can be used to calibrate all elements of pellet fuelling physics such as: the pellet ablation process, prompt pellet material loss due to ELMs, redistribution of pellet material due to grad-B drift and post-pellet density and isotope mix evolution. In particular while fuelling pellets are used to fuel the plasma and control the density, they can also trigger ELMs, which affects the pellet fuelling efficiency. Detailed analysis of this kind will be the subject of separate paper.

## 2. Experimental set up

The plasma used in this study belongs to the so-called baseline scenarios that are predicted to achieve  $Q=10$  in ITER at 15MA. These plasmas are defined by a safety factor at the edge of  $q_{95} = 3$  and  $q_0 < 1$  on the axis. For a detailed description of baseline D-T plasmas on JET see the recent paper [6]. For this study, the plasma current was  $I_p = 3.0$  MA, toroidal magnetic field  $B_T = 2.9$  T, safety factor  $q_{95} = 3.1$ . The plasma used a low triangularity  $\delta_{U,L} = 0.12/0.27$  configuration with a divertor optimized for pumping, which is known to be beneficial for access to good H-mode confinement [6]. A similar scenario was used for the DTE2 experiments where the tritium was supplied by gas puffing and with half of the neutral beams reaching an isotope mix of 50%-50%, both at the edge and also in the core. This was confirmed by a TRANSP evaluation of the neutron rate [6].

JET is equipped with pellet injector which can deliver deuterium pellets from the top of the machine on the

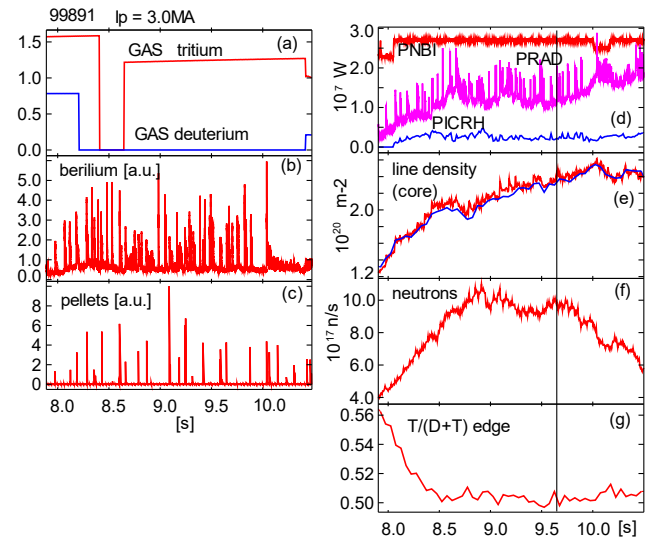


**Figure 1.** Overview of the main shot analysed in this paper study. (a) gas flow rates, (b) Be light emission, (c) pellet ablation light, (d) neutral beams, RF heating and bolometer emission power, (e) core line-integrated density from interferometry (red) and from Thomson scattering (blue), (f) total neutron rate, (g) isotope mix ratio at the edge.

high field side with a velocity of  $\sim 150$  m/s. Two pellet sizes can be used. Firstly small pellets (diameter of 2mm, length 2mm, volume  $6.3\text{mm}^3$ ) can be used for ELM pacing [6], thus allowing stable ELMy H-mode, while at the same time avoiding W accumulation [6]. Secondly, an injector can deliver large pellets (diameter of 4 mm, length of 3.2mm, volume  $40\text{mm}^3$ ), for plasma density and isotope mix control, though only deuterium pellets are available.

An example of the scenario used to test pellets to control the isotope mix in D-T plasmas is depicted in figure 1. As shown in the figure, the D gas puffing is switched off at  $t=8.2$  s and D is only provided by the D fuelling pellets during the main heating phase. In this case, the pellet fuelling rate was 12Hz and the D-T ratio reached a stable 50%-50% value for  $\sim 1.5$  s. This phase, during which the radiated power remains stationary and the plasma effective charge  $Z_{eff}=1.8$ , is terminated by an unintended pause in pellet train after 9.85 s and a subsequent transition to an ELM free phase, resulting in core impurity accumulation followed by the termination of the H-mode. This is the best pulse achieved in this experiment. We call the pulse the “reference” plasma.

## 3. Scan of isotope mix and pellet frequency

From the control point of view it is useful to compare the reference plasma described above with plasmas where two

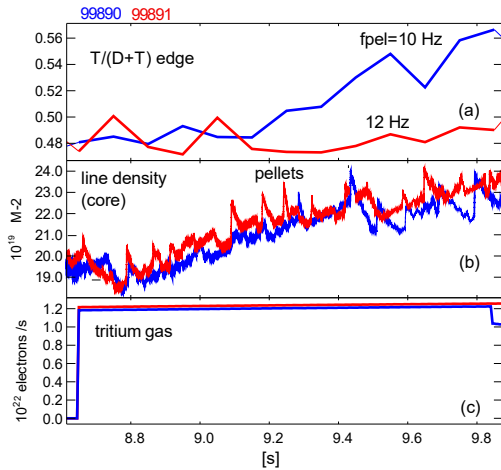


**Figure 2.** Effect of pellet rate on isotope mix ratio. (a) isotope mix ratio from edge spectroscopy, (b) core line-integrated density, (c) tritium gas flow.

main actuators, isotope mix and pellet frequency, changed independently.

Sensitivity to pellet frequency is shown in figure 2 where pellet frequency is reduced from 12Hz to 10Hz, while all other parameters are the same as in the reference plasma. It is seen that a 10 Hz pellet rate is too small to keep the isotope mix constant at a 50%-50% value. This scan also quantifies that in order to change the D-T mix ratio by 16% around the 50%-50% value the pellet rate should change by 20%.

The importance of the isotope mix is explored in a further comparison of the reference D-T plasma with a pure D plasma (see shot 99891 vs 94756 in figure 3a, b). The pellet fuelling size and rate, and the gas fuelling rate ( $1.1 \times 10^{22}$  e1/s) were similar to that in the reference pulse but the NBI heating power was somewhat lower than in the reference shot (21MW). The electron temperatures at pedestal top are similar. The main difference between these two plasmas is the higher density in D-T pulse compared to pure D plasma. If this difference in densities would be related solely to the change of effective mass then the plasma density would scale as  $n_e \propto M_{eff}^{0.62}$ . This however is not the full picture. Visual inspection of interferometer signal shows that the density decay after individual pellets is faster in D plasma compared to D-T plasma (for one pellet cycle see the shaded time intervals in figures 3a,b). As will be discussed later, the pellet particle loss is controlled by ELMs and thus the lower density in the D case can be attributed to a higher ELM frequency. If the reduction of plasma density is fully due to the ELM frequency, then the density would scale as  $n_e \propto f_{ELM}^{-0.41}$ .

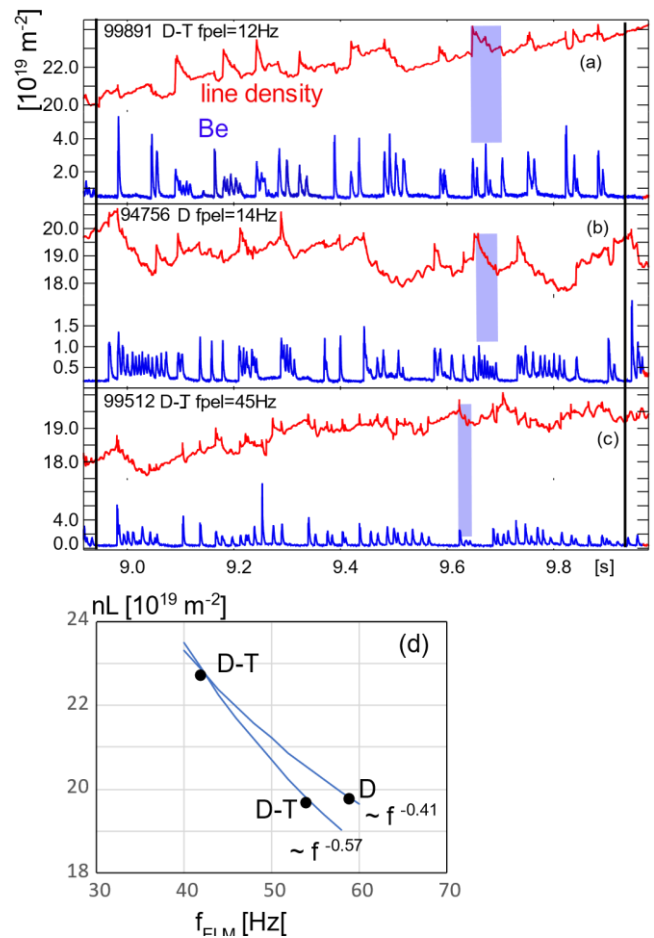


**Figure 3.** Comparison of reference pulse (D-T plasma, fuelling D pellets, panel a) with two plasmas in which, first, isotope content was pure D (panel b) and, second, with D-T plasma ELM pacing pellets (panel c). For each plasma two signals are shown: the core line integrated density from interferometer (red) and the ELM signal as seen on Be light emission (blue). The shaded areas show the examples of single pellet cycles discussed in the text. Panel (d) shows the dependence of line integrated density on ELM frequency calculated from reference shot on panel (a) and two plasmas on panels (b) and (c). The ELM frequencies and line densities are both averaged over the interval shown by two black vertical lines in panels (a, b, c). The line densities are calculated from Thomson scattering profiles.

Finally the impact of pellet size is explored by comparing the reference D-T plasma with  $40\text{mm}^3$  pellets with D-T plasma where throughout the whole pulse the pellet size was reduced to  $6.3\text{mm}^3$  and pellet rate increased to 45Hz (see shot 99891 vs 99512 in figure 3a, c). The NBI power (25MW), gas rate ( $0.7 \times 10^{22}$  e1/s), pedestal temperature and isotope mix ratio

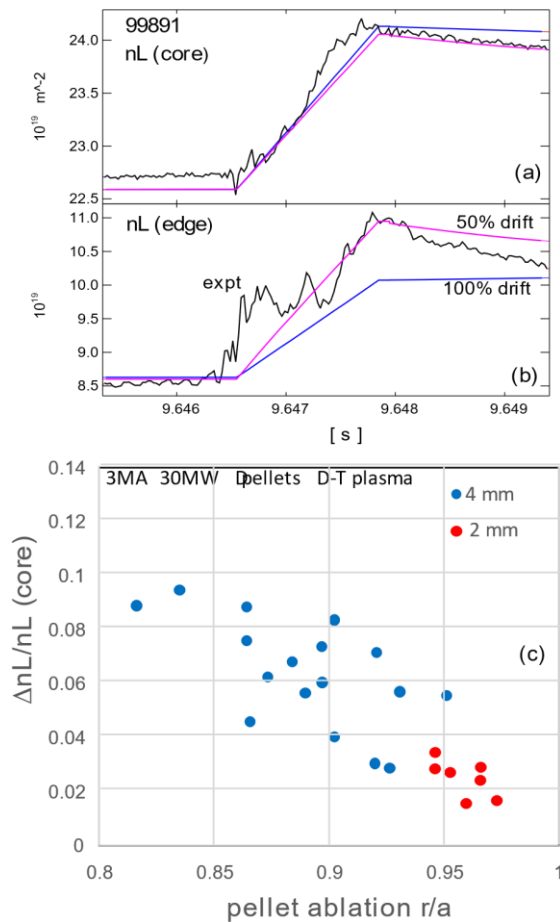


**Figure 4.** Comparison between measured and modelled (HPI2) temporal evolution of the (a) core and (b) edge ( $r/a=0.9$ ) line integrated density measured by two vertical interferometer channels during pellet deposition. Two values of plasmoid drift are used. (c) The dataset of pellets showing the correlation between pellet ablation radius and relative perturbation of line integrated density. The pellet deposition radius is calculated from nominal pellet velocity and pellet deposition time interval.

were similar to that in the reference shot. The main difference between these plasmas is the lower density in the shot with small high frequency pellets. The reason is that these small pellets act as an ELM controller while the fuelling efficiency is low. If the reduction of plasma density is fully attributed to ELM frequency then the density would scale as  $n_e \propto f_{ELM}^{-0.57}$ .

These two dependences of plasma density on ELM frequency are summarised in figure 3(d). It is seen that in both cases the dependence is very similar. This is interesting because the mechanism behind the increase of ELM frequency in these two cases is different (the change of mass ratio vs. pellet ELM pacing). As it is seen in figure 3d the ELM

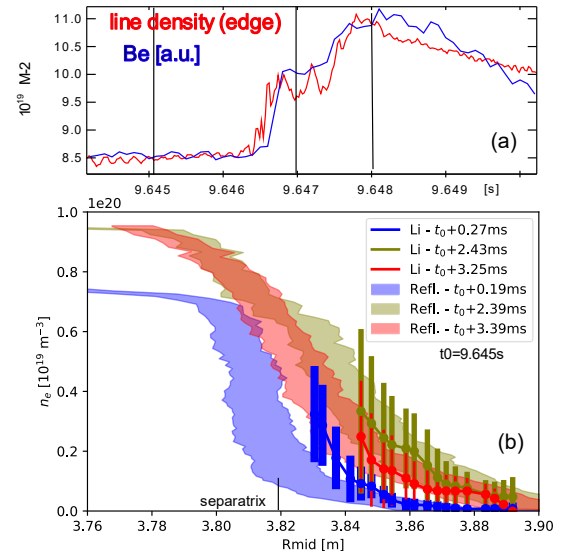


**Figure 5.** Prompt losses documented by reflectometer and Li beam spectroscopy. Pulse no 99891. (a) temporal evolution of edge interferometer signal and Be light emission. (b) Density profiles at times marked in panel (a) as measured by reflectometer and Li beam spectroscopy.

frequency is higher than pellet frequency. In addition each pellet triggers an ELM. This is the case for both pellet sizes. For fuelling pellets the correlation between pellet and prompt and post-pellet ELMs will be discussed in the next sections.

#### 4. Pellet deposition and prompt pellet losses

When a pellet enters the plasma it evaporates, ionises and deposits at the plasma periphery. How much and where the pellet is finally deposited depends on the intensity of inward drift of discrete plasmoids emanating from pellet and size of prompt outward losses. The overall pellet efficiency depends on both of these two processes. By “prompt” we refer to losses of the plasma when the pellet deposition takes place. Regarding the neutral cloud it is permanently located in the small vicinity of the pellet and thus is not directly participating in particle losses.

Figure 4 (a, b) shows the evolution of plasma density following a single pellet as measured by fast interferometer signals. Pellet deposition interval is clearly marked by the change of slope events. The experimental data are compared with the simulation using the JINTRAC suite of codes [7, 8, 9] that uses the HPI2 code [10, 11] to model the pellet ablation and deposition. In order to get agreement with the core line integrated density the pellet size has to be reduced from the nominal value at the pellet injector. This difference is attributed to the losses in the flight line. After the reduction the density increase and also duration of the pellet deposition

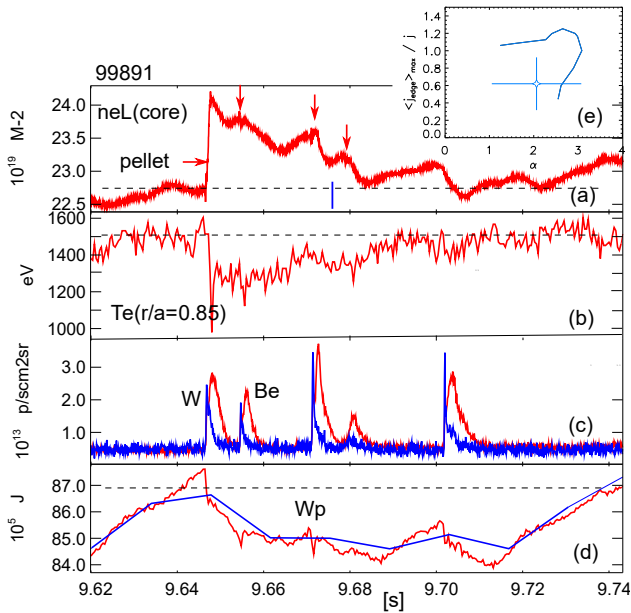


**Figure 6.** Post pellet losses in full pellet circle. (a) core line integrated density, (b) Electron density at the plasma periphery, (c) W (blue) and Be (red) emission, (d) energy content from slow (blue) and fast (red) equilibrium reconstruction. The insert of ideal MHD analysis refers to the time indicated by blue vertical bar in top panel.

process are well simulated by the code. The agreement between the code and the experiment is less satisfactory for the edge interferometer signal. The agreement can be broadly restored by reducing the plasmoid drift velocities by 50% as seen in figure 4(b). We need clarification in this observation as ITER relies on plasmoids drift for efficient fuelling.

The core interferometer signal described above is used to create the dataset of individual pellets as seen in figure 4 (c). The pellet ablation depth is calculated from the duration of pellet deposition phase and from nominal pellet velocity. The variation of ablation depth can be explained by some variability of pellet sizes already observed at the pellet injector combined with uncontrolled flight tube losses. The vertical axis shows the relative perturbation of core interferometer signal due to pellets. It is seen that the size of density perturbation decreases as pellet ablation depth becomes more peripheral. This is consistent with increasing prompt pellet loss for shallower pellets. Note that in ITER pellet ablation radius is expecting to be  $r/a \sim 0.95$ .

After indication that prompt pellet losses could be significant we inspected a single pellet event in more detail. Figure 5a shows the edge interferometer and Be light emission signals. It is seen that an increase of plasma density due to pellet deposition happens at the same time as the increase of

Be light. The evolution of density profiles before, during and at the end of pellet ablation, as measured by Li beam spectroscopy and reflectometry, is shown in figure 5b. It is seen that the prompt loss event manifests itself as  $\sim 2\text{cm}$  outward shift of the edge density profiles at 9.647s and 9.648s) relative to the pre-pellet profile at 9.645s. If the shift is interpreted as a plasma moving into the region with open field lines then this loss consists of  $\sim 2 \times 10^{20}$  el. This amount is about  $\sim 20\%$  of the pellet size as determined from the edge interferometer signal using pellet deposition code, or in other words pellet fuelling efficiency at plasma is  $\sim 80\%$ . This prompt particle loss, synchronised with the increase of Be light emission, is similar to conventional ELM. Also all fuelling pellets injected into H-mode show the aforementioned phenomenology. Nevertheless the co-existence of ELM with an ablating pellet could mean that some relevant differences could exist between natural and pellet triggered ELMs. For example the dependence of pellet triggered ELMs on pellet size could have a strong impact on modelling for ITER.

## 5. Post pellet transport

After pellet deposition the plasma density starts to decrease and after a certain time it reaches the pre-pellet value and next pellet can be injected. Figure 6 shows the temporal evolution of plasma during one pellet cycle. It is seen that the plasma density reaches the pre-pellet value in  $\tau_{pel} \sim 60\text{ms}$  or  $\tau_{pel}/\tau_E \sim 0.2$ , when normalised by energy confinement time. At the same the peripheral electron temperature drops during the pellet deposition and then recovers to pre-pellet value, synchronously with plasma density. Plasma energy content  $W_p$  recovers to pre-pellet value in  $\tau_{pel} \sim 90\text{ms}$ , somewhat longer than peripheral electron density and temperature, that could be due to the pressure profile effects. As mentioned above, plasma density decreases during the post pellet interval. This decrease is not monotonic but occurs in multiple separated phases. Each phase is triggered by a short ELM-like event manifested by a burst of W and Be line radiation. In addition, small oscillations might be visible on interferometer signal as indicated by arrows in figure 6(a). To test whether these bursts are caused by an ideal MHD instability a conventional  $j$ - $\alpha$  analysis was performed. It is seen in figure 6(e) that during the pellet cycle plasma is expected to be stable against ideal peeling or ballooning modes and another different mechanism might be in place.

ELM events mentioned above are followed by a phase of decreasing plasma density which we interpret as L-mode. These L-mode phases last about 5-10ms, clearly longer than the bursts of W emission or oscillations on fast interferometer signal. Therefore the post pellet losses are mostly controlled by the duration of L-mode phases rather than by the amplitude of ELMs. The L-mode phases are

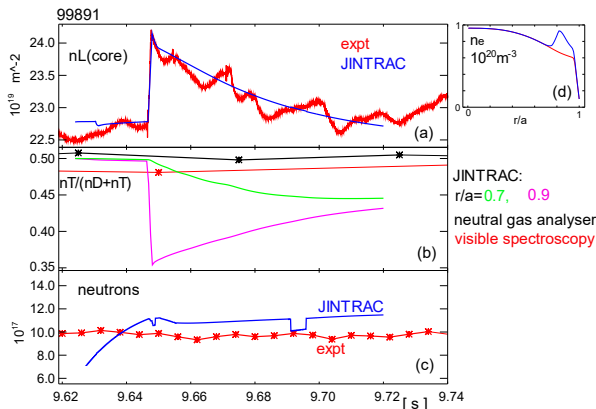


**Figure 7.** Modelling of post pellet phase by JINTRAC code. (a) line integrated density, (b) edge isotope mix ratio from: visible spectroscopy (red), neutral gas analysis in divertor (black) and JINTRAC code (green and pink), (c) neutron rate from experiment (red) and from JINTRAC (blue), (d) electron density profile before and after pellet injection calculated by JINTRAC.

terminated by spontaneous transitions to H-mode as indicated by increasing density, temperature and energy content.

Finally note that the elements of the pellet cycle described above are quite generic and we observed such phenomenology in another experiments e.g. in H-D plasma in JET [12]. In particular the fact that the post-pellet density decay time scales broadly with energy confinement time is encouraging as this can be used for extrapolation towards ITER.

## 6. Modelling

Pellet deposition and post pellet particle transport was modelled by JINTRAC code. The purpose of this simulation is similar to our previous analysis of H-D plasma [12], namely to validate particle transport model. This is done by evolving deuterium and tritium densities while temperature is taken from experiment. The code then calculates the relevant diagnostic signals and compare them with available experimental data. The process is iterative during which the parameters of particle transport model are changing. In our case these parameters are the ratios between particle and heat diffusivities where heat diffusivities are taken from the Bohm-gyroBohm transport model. For details see our previous paper [12].

An example of such a simulation is shown in figure 7(a). It is seen that during the pellet cycle the line averaged

density is well fitted by the simulation. After the pellet deposition the perturbation of the density decays and reaches  $1/e$  value at 9.67s. At this time the particle flux at the top of the pedestal  $r/a = 0.95$  is  $\Phi = 1.1 \times 10^{22}$  at/s or  $\Gamma/ne = 1.1$  m/s. Note that 88% of this particle flux is due to  $dN/dt$  term. This particle flux can be related to the heat flux through the pedestal  $Q$  such as:  $\Phi T/Q=0.040$ , where  $T=455eV$  and  $Q=20MW$  are the temperature and heat at the top of the pedestal. Such a fraction of convective particle flux well compares with other pellet fuelling experiments as seen in table 1. Finally note that in ITER modelling this fraction is usually assumed to be close to the value in our experiment. These data could help to build a simple law to predict pellet fuelling throughput for next fusion reactors.

Figure 7(b) shows the evolution of isotope mix ratio at the plasma periphery as modelled by JINTRAC code. It is seen that in our case of injection of deuterium – tritium plasma, the modulation of isotope mix is significant. It is also seen that this modulation is not captured by edge diagnostics, likely due to insufficient temporal and spatial resolution.

Figure 7b also shows that the modulation of isotope mix ratio becomes smaller towards the plasma centre. This is consistent with the negligible modulation of experimental neutron rate in figure 7c and is confirmed by JINTRAC simulation.

Extrapolating these observations to ITER, with separate deuterium and tritium pellets, the modulations of plasma effective mass due to alternating D and T pellets could cause unwanted oscillations of energy confinement. This raises the question whether the pre-mixed D-T fuelling pellets should be used in ITER and what fraction of tritium should be separated in the outer loop of the system. The answer to this question depends on detailed physics basis of interaction of pellets with various parts of the plasma. In addition pre-mixed H-D fuelling pellets in Asdex Upgrade (AUG) were used to

**Table 1.** Pellet fuelling throughput and  $\Phi T/Q$  parameter for selected experiments.

Machine /experiment	Pellet flux [ $10^{21}$ at/s]	$\Phi T/Q$	Ref
AUG/RMP	1.9	0.050	[14]
AUG/RMP	5.6	0.073	[13]
JET/H:Dcontrol	8.2	0.043	[12]
JET/DTbaseline	11	0.040	this expt
ITER/baseline	7.7	0.050	[2] tab. 4E

address the problem showing that it should be part of fuelling scheme [15].

## 7. Conclusions

A dataset of baseline D-T plasmas with HFS fuelling pellets has been produced on JET. The pellet deposition and pellet relative size is similar to those expected in ITER. This is the unique property of this dataset that allows a calibration of many elements of physics basis of pellet fuelling under relevant conditions expected in ITER. This paper presents the data achieved so far with some initial findings that need to be confronted with present models. The underlying feature of this comparison is the fact that pellets are peripheral with complex interaction between pellet deposition/retention and plasma particle transport, including ELMs. The main findings in this paper related to particular elements of pellet fuelling physics basis are listed below:

- The model of pellet ablation in the HPI2 code can give a reasonable fit to the experiment, only if the modelled drifts are artificially reduced.
- During the pellet ablation phase prompt particle losses due to pellet triggered ELMs can be detected.
- Post pellet particle losses are controlled by “compound ELMs”, i.e. transient L-mode phases triggered by ELMs. Post-pellet particle loss, normalised to heat flux, is in good agreement with pellet fuelling experiments on AUG and JET.

## Acknowledgements

This work has been carried out within the framework of the EUROfusion Consortium, funded by the European Union via the Euratom Research and Training Programme (Grant Agreement No 101052200 — EUROfusion) and from the EPSRC [grant number EP/W006839/1]. To obtain further information on the data and models underlying this paper please contact [PublicationsManager@ukaea.uk](mailto:PublicationsManager@ukaea.uk)\*. Views and opinions expressed are however those of the author(s) only and do not necessarily reflect those of the European Union or the European Commission. Neither the European Union nor the European Commission can be held responsible for them. Authors would like to thank to Drs. S. Henderson, C. M. Roach and L. Warwick for reading the manuscript and valuable comments.

## References

- [1] M. Lennholm et al 2021 *Nucl. Fusion* **61** 036035
- [2] Polevoi A *et al* 2018 *Nucl. Fusion* **58** 056020
- [3] Lang P T et al, *Phys. Rev. Lett* **79** 1997
- [4] Baylor L *et al* *Bulletin of the American Physical Society*, Volume 63, Number 11, 60th Annual Meeting of the APS Division of Plasma Physics November 5–9, 2018; Portland, Oregon, UP11.00049
- [5] ITER research plan, items B.2.8 “Fueling of peripherally deposited pellets” and B.2.18 “T and D transport and DT mix control by peripheral pellet fuelling”
- [6] Garzotti L. et al. 2023 *Nucl Fusion* this issue
- [7] Romanelli M et al (JET EFDA Contributions) 2014 JINTRAC a system of codes for integratind simulations of tokamak scenarios *Plasma Fusion Res.* **9** 3403023
- [8] Garzotti L. *et al.* 2012 *Nucl Fusion* **52** 013002
- [9] Parail V. *et al* 2009 *Nucl. Fusion* **49** 07503
- [10] Koechl F et al Modelling of Pellet Particle Ablation and Deposition : The Hydrogen Pellet Injection code HPI2, EFDA-JET-PR(12) 57 (2012)
- [11] Pegourie B et al. 2007 *Nucl Fusion* 47 44
- [12] Valovič M. et al 2019 *Nucl. Fusion* 59 106047
- [13] Valovič M. et al 2016 *Nucl. Fusion* 56 066009
- [14] Valovič M. et al 2018 *Plasma Phys. Control. Fusion* **60** 085013
- [15] Lang P.T et al 2019 *Nucl. Fusion* 59 02600